

Article

# Photocatalytic Degradation of a Systemic Herbicide: Picloram from Aqueous Solution Using Titanium Oxide (TiO<sub>2</sub>) under Sunlight

Md. Rakibul Islam <sup>1</sup>, Jahida Binte Islam <sup>1,\*</sup> , Mai Furukawa <sup>1</sup>, Ikki Tateishi <sup>2</sup>, Hideyuki Katsumata <sup>1</sup>  and Satoshi Kaneco <sup>1,2,\*</sup> 

<sup>1</sup> Department of Chemistry for Materials, Graduate School of Engineering, Mie University, Tsu 514-8507, Japan; rakibulislamlikhon@gmail.com (M.R.I.); maif@chem.mie-u.ac.jp (M.F.); hidek@chem.mie-u.ac.jp (H.K.)

<sup>2</sup> Global Environment Center for Education & Research, Mie University, Tsu 514-8507, Japan; tateishi@gecer.mie-u.ac.jp

\* Correspondence: jbislam07@gmail.com (J.B.I.); kaneco@chem.mie-u.ac.jp (S.K.); Tel.: +81-59-231-9427 (J.B.I.)

Received: 30 June 2020; Accepted: 9 October 2020; Published: 27 October 2020



**Abstract:** The photocatalytic degradation of picloram (4-amino-3,5,6-trichloro-2-pyridincarboxylic acid), which is one of popular acidic herbicide, was investigated with the existence of titanium oxide (TiO<sub>2</sub>) under sunlight. The total photocatalytic degradation of 20 ppm of picloram was occurred within 30 min irradiation with TiO<sub>2</sub>, while a negligible degradation was found without TiO<sub>2</sub> under sunlight. The influence of various parameters, like TiO<sub>2</sub> dosage, solution initial pH, intensity of light, reaction temperature and irradiation time, was found during the photocatalytic degradation of picloram. The mineralization of picloram was proved by the deterioration of total organic carbon (TOC) of the photocatalytic process. The pseudo-first order kinetics of photocatalytic degradation was obtained according to the Langmuir–Hinshelwood model, and the reaction rate constant was  $17.6 \times 10^{-2} \text{ min}^{-1}$ . Chloride ion, ammonium ion, nitrate ion and CO<sub>2</sub> were erected as the final products after completing the photocatalytic degradation of picloram. The intermediate products could not be determined by the GC–MS during the degradation of picloram. Therefore, the degradation mechanism of the picloram was proposed based on the frontier electron density and the point charge at each atom of the picloram molecule. The photocatalytic degradation method, using sunlight, may develop into as a pragmatic technique to purify picloram contaminated wastewater.

**Keywords:** picloram; photocatalytic degradation; titanium oxide; mineralization; total organic carbon

## 1. Introduction

Picloram (4-amino-3,5,6-trichloro-2-pyridincarboxylic acid) is a systemic translocation-possible and hormone herbicide used to control the annual and perennial broadleaf plant such as mugwort, dockweeds, thistles, bramble and Japanese Knotweed, which are normally found in pasture and rangelands [1]. Picloram is a chlorinated derivative of picolinic acid containing a pyridine ring [2]. The molecular structure of the picloram is shown in Figure 1. Picloram herbicide is selectively absorbed through the roots, stems and leaves of target weeds. Picloram is the most persistent herbicides of its family, with half-lives from 20 to 300 days, depending on the soil quality [3,4]. Picloram scarcely adhere to soil and highly soluble in water (430 mg/L at 25 °C). Its degradation slowly occurred in soil, however no volatilization was found [5,6]. Picloram can be drained by the rainfall action and reach toward the surface and underground water, and ultimately, contaminated water. Moreover, air, soil and biomass can also be contaminated when picloram comes in contact with the environment [7]. Chronic exposure of picloram to wildlife is a matter of concern because of the persistence of picloram in nature.

Normally, birds, mammals and aquatic species are not affected by picloram, but some transformation products of picloram could be toxic when inhaled and splashed into the eyes. In addition, the weight loss and liver damage in mammals due to long-term exposure to high concentration of picloram is reported in many studies [8,9]. Therefore, remediation of picloram contamination should be considered. Generally, photolysis [10], Fenton reactions [11], electro-Fenton reaction [3], photo-Fenton reaction, chemical oxidation and hydrolysis [12], bio-sorption [13] and biodegradation [14] traditional methods have been implemented to detoxify picloram containing wastewater. Regrettably, these classical strategies have various shortcomings, like being costly, ineffective and generating secondary pollutants directly, and eventually, being responsive to the environmental pollution. On the contrary, high efficiency and low energy loss are advantageous characteristics of the photocatalytic degradation technology. The cost effectiveness and easy application makes this technique quite alluring to degrade toxic substances [15,16]. The photocatalytic technique associates the transfer of the valence band (VB) electrons to the conduction band (CB) of the photocatalyst under light irradiation, which have higher energy photons than its bandgap, and holes remain in the valence band. Some common semiconductor based photocatalysts are universally practiced because of the stable chemical properties, and favorable bandgap energy to be excited under ultraviolet (UV) irradiation or solar irradiation [17–20]. Amid them all,  $\text{TiO}_2$  is extensively used due to the suitable bandgap ( $E_g = \sim 3.20 \text{ eV}$ ), nontoxicity, low cost, and high photosensitivity [21]. However, the low chemical stability of photocatalysts, except for  $\text{TiO}_2$  in strong acidic solution, is also a recognized drawback parallel to all advantages [22]. Moreover, photocatalysts can be recycled and repeatedly reused after completing photocatalytic degradation [23]. The number of research works on the photocatalytic picloram degradation under UV or solar irradiation using  $\text{TiO}_2$  is still limited today [2,24–26]. Moreover, the photocatalytic treatment under sunlight is reasonable, smooth and eco-friendly rather than that of applying artificial light sources like LED, black, and Hg–Xenon lamp. Therefore, the photocatalytic degradation of the picloram with  $\text{TiO}_2$  under sunlight could be designed as an impressive strategy to decontaminate picloram from wastewater.

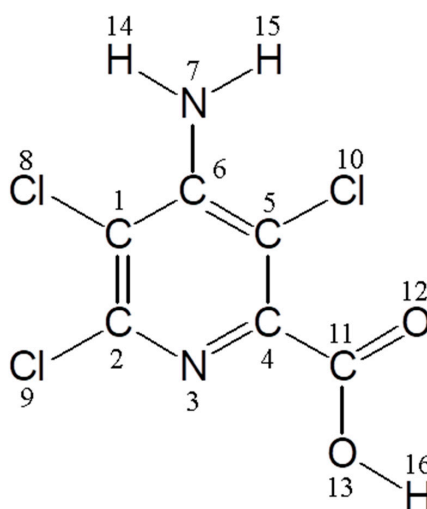


**Figure 1.** Molecular structure of picloram (4-amino-3,5,6-trichloro-2-pyridincarboxylic acid).

The current research manifests the photocatalytic degradation of picloram in aqueous solution with nanosized  $\text{TiO}_2$  under sunlight. The intermediate products of picloram were determined by the gas chromatography-mass spectroscopy (GC/MS). A plausible reaction mechanism has been delineated owing to the generation of intermediate products and final products of picloram. The various parameters, for example,  $\text{TiO}_2$  dosage, solution pH, reaction temperature, intensity of sunlight and irradiation time have been amended for the highest photocatalytic degradation of the picloram.

## 2. Experimental Section

### 2.1. Chemicals and Materials

Picloram ( $C_6H_3Cl_3N_2O_2$ ) was obtained from FUJIFILM Wako Pure Chemical Industries Ltd., Osaka, Japan.  $TiO_2$  (P-25) was bought from the Nippon Aerosil Co. Ltd., Tokyo, Japan. Methanol ( $CH_3OH$ ), potassium hydrogen phthalate ( $C_6H_4(COOH)(COOK)$ ), sodium carbonate ( $Na_2CO_3$ ), dichloromethane ( $CH_2Cl_2$ ), sodium bicarbonate ( $NaHCO_3$ ), and ammonium chloride ( $NH_4Cl$ ) were purchased from the Nacalai Tesque Co. Ltd., Kyoto, Japan. Acetonitrile was bought from Kanto Chemical Co., Tokyo, Japan. HCl and NaOH were used to adjust the solution pH.

### 2.2. Photocatalytic Degradation of Picloram

The needed amount of picloram powder was mixed with ultrapure water to prepare 20 ppm stock solution of picloram. An ultrapure water device (GSH-2000; Advantech Co., Ltd. Tokyo, Japan) provided this ultrapure water. For a conventional photocatalytic experiment, 30 mL of 20 ppm picloram solution was shifted into a 50 mL Pyrex vessel, and 300 mg  $TiO_2$  nanopowder was dissolved into the picloram solution. The reaction temperature was constant at 25 °C using a water bath. The  $TiO_2$  containing picloram solution was regularly stirred by a magnetic stirrer for 30 min in the dark to reach the adsorption–desorption equilibrium, and the suspension was continuously stirred throughout the experiment for the dispersion of  $TiO_2$  after solar irradiation. The short ultraviolet radiation ( $\lambda < 300$  nm) was filtered by the vessel wall. A UV intensity meter having a sensor of 230 nm to 400 nm wavelengths (UVR-400; AS ONE Co., Tokyo, Japan) was applied to measure the irradiance. The experimental set up was shown in Figure 2.

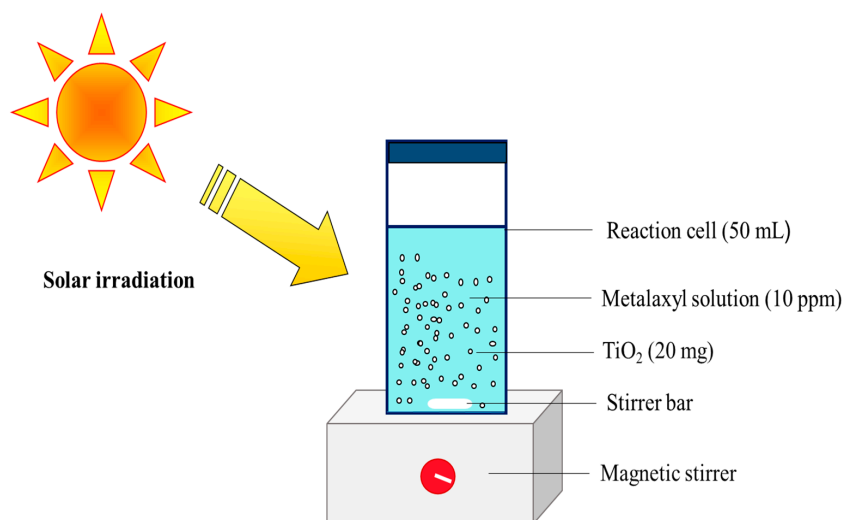


**Figure 2.** Experimental set up of the photocatalytic degradation of picloram with  $TiO_2$  under sunlight.

$TiO_2$  was removed by the 0.45  $\mu m$  Advantec membrane filter after irradiation. A high-performance liquid chromatograph containing a UV optical detector and ODS-3 (5  $\mu m$ ) (Varian, Tokyo, Japan) column was applied to measure the picloram concentration in aqueous solution. The elution was recorded at 220 nm. The eluent was the mixture of acetonitrile and water (50/50,  $v/v$ ), and the flow rate was 1  $mL \cdot min^{-1}$ . The volume of the inserted sample was 20  $\mu L$ . After that, the concentration of converted  $NH_4^+$  and  $Cl^-/NO_3^-$  ions were estimated by an anion ion chromatography after removing  $TiO_2$  from the picloram solution. Summarized experimental conditions were exhibited in Tables S1 and S2. The photocatalytic degradation efficiency of picloram was computed by the following equation:

$$\text{Degradation efficiency of picloram (\%)} = \frac{C - C_0}{C_0} \times 100 \quad (1)$$

where  $C_0$  and  $C$  are the concentration of picloram before and after degradation.

The mixed gas ( $O_2 + N_2$ ) was run for 30 min to eliminated inorganic carbon from the picloram solution and finally, the total organic carbon (TOC) was determined by Shimadzu TOC analyzer (TOC-VE). The standard solution of potassium hydrogen phthalate to get the calibration curve TOC.

Molecular orbital (MO) computations were executed at the single determinant (Hartree–Fock) level to optimize the minimum energy gained at the AM1 level. All the semi-empirical calculations were conducted in MOPAC (Version 6.01) along a CAChe package (Fujitsu Co. Ltd. Tokyo, Japan). The point charge and the frontier electron density at each atom of the picloram molecule were evaluated. The solid-phase extraction gas chromatography and mass spectroscopy (GC-MS) were used to determine the intermediate products, which are obtained during the degradation of picloram. A Shimadzu gas chromatography mass spectroscopy (GCMS-QP5000, Shimadzu, Kyoto, Japan) was furnished with a CP-Sil 8 CB capillary column. The chromatographic criteria was shown in Table 1.

**Table 1.** The analytical conditions for GC-MS.

Capillary column	CP-Sil 8 CB ( $\varphi = 0.25 \text{ mm} \times 30 \text{ m}$ )
Column temperature program	$50 \text{ }^\circ\text{C} (1 \text{ min}) \Rightarrow \text{up } 15 \text{ }^\circ\text{C/min} \Rightarrow 280 \text{ }^\circ\text{C} (10 \text{ min})$
Injector temperature	$280 \text{ }^\circ\text{C}$
Interface temperature	$280 \text{ }^\circ\text{C}$
Carrier gas	He (99.9%), 81.6 mL/min
Ionization	Electron- impact (EI) mode
Injected volume	$1 \text{ } \mu\text{L}$

### 3. Results

#### 3.1. The Changes of UV-Vis Spectra

The UV absorption spectrum change has been investigated to confirm the photocatalytic picloram decomposition with  $TiO_2$  under UV irradiation over the range of 200 to 300 nm, employing a UV-Vis spectrophotometer. The specific experimental conditions are given in the Supplementary Material (Table S3). According to Figure 3, the picloram exhibits a major absorption band at 225 nm before light irradiation (curve a). Moreover, the same absorption peak was found in the absence of  $TiO_2$  after 10 min of solar irradiation (curve b). However, a well-established absorption band intensity was reduced after 10 min of solar irradiation with  $TiO_2$ , explaining that picloram could be photocatalytically degraded by  $TiO_2$  under sunlight (curve c). It was concluded that the picloram does not decompose in the absence of  $TiO_2$  under sunlight.

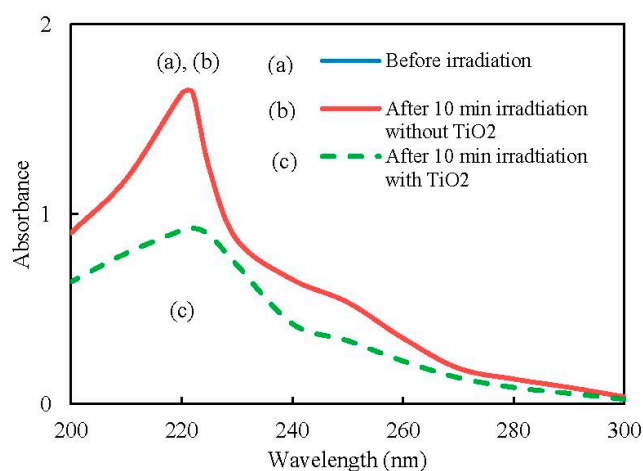


**Figure 3.** UV-visible spectral changes of picloram before and after UV irradiation.

### 3.2. Influence of TiO<sub>2</sub> Dosage

The influence of TiO<sub>2</sub> dosage on the photocatalytic degradation of the picloram has been scrutinized by varying TiO<sub>2</sub> amounts from 0 to 500 mg. The consequences are presented in Figure 4. The degradation efficiency was gradually increased with an increasing TiO<sub>2</sub> amount up to 300 mg, and the same pattern of the result was observed for the further addition of TiO<sub>2</sub> above 300 mg. Similar phenomena have been shown for the degradation of other organic compounds [27]. A large amount of photocatalyst could turbid the reaction solution, and therefore, the penetration of light could be hindered. In addition, a loss of active surface area could be occurred due to agglomeration (particle-particle interactions) at higher concentrations of the photocatalyst. As a result, the percentage of degradation did not increase due to the lack of light penetration [28]. Therefore, 300 mg TiO<sub>2</sub> was chosen as the optimal dosage for further analysis.

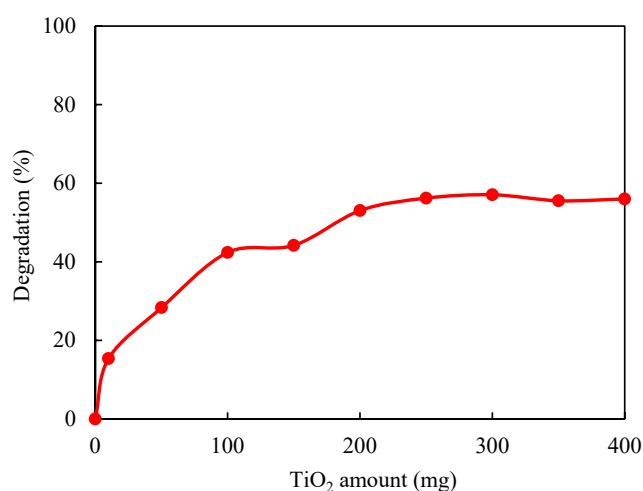


**Figure 4.** Influence of TiO<sub>2</sub> dosage on the photocatalytic picloram degradation in existence of TiO<sub>2</sub> under sunlight. Picloram: 20 ppm; irradiation time: 10 min; pH: 4; intensity of light: 1.8 mW/cm<sup>2</sup> and temperature: 30 °C.

### 3.3. Influence of pH

The solution pH is an important factor during the photocatalytic treatment process because of the variation of surface charge of the photocatalyst with the solution's initial pH. Hence, the influence of initial pH on the photocatalytic degradation of the picloram with TiO<sub>2</sub> under 10 min sunlight was investigated, changing the pH from 2 to 12. The solution's initial pH was not adjusted during the experiment, and the pH was four. As seen in Figure 5, the photocatalytic degradation efficiency of the picloram was decreased with higher pH. Briefly, the highest 62% degradation efficiency was observed at pH 8, but the efficiency declined sharply above pH 8. When the pH is lower than the point of zero charge of nanosized TiO<sub>2</sub> (pzc = 6.5), the TiO<sub>2</sub> surface becomes positively charged as Ti<sup>IV</sup>-OH<sup>2+</sup>, this condition is favorable to the photocatalytic picloram degradation [29]. Again, the picloram has a carboxyl group (-COO<sup>-</sup>), which is negatively charged and could repel the negatively charged TiO<sub>2</sub> surface at higher pH levels. Consequently, degradation efficiency declined in the basic condition. In addition, there is no significant change in degradation efficiency from the acidic range to the neutral range. The results confirmed that the more efficient degradation of the picloram can be obtained in the experiment conducted in the acidic to the neutral range of pH. Therefore, pH 4 was selected as the optimum pH, and pH adjustment was not needed for the experiment.

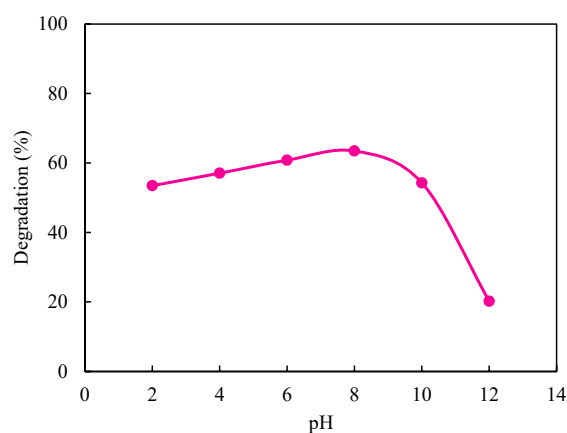


**Figure 5.** Influence of initial pH on the photocatalytic picloram degradation in existence of  $\text{TiO}_2$  under sunlight. Picloram: 20 ppm;  $\text{TiO}_2$ : 300 mg; irradiation time: 10 min; intensity of light:  $1.8 \text{ mW/cm}^2$  and temperature:  $30^\circ\text{C}$ .

### 3.4. Influence of Intensity of Light

The solar photocatalytic treatment is related to the intensity of sunlight, and it is immensely dependent on the weather, latitude, season, and time of the treatment place. Assuming these factors, the determination of influence of the light intensity on the photocatalytic picloram degradation with  $\text{TiO}_2$  is essential. The photocatalytic picloram degradation was performed under sunlight with various intensities of light at different times of cloudy and sunny days. As presented in Figure 6, the degradation efficiency of picloram was steadily raised as the intensity of light raised. Stereotypically, photocatalyst absorbs the photon energy from the irradiated light with an equal or more than bandgap energy. The separation of electron-hole in photocatalyst could be improved by hiking the irradiated light intensity [30]. Consequently, the degradation of picloram is low at a low intensity of light owing to the number of excited electrons. In addition, the recombination of hole-electron is a normally assumed limitation in photocatalysis. The separation of hole-electron pair struggles at lower light intensity, which lessens the free radicals generation, and eventually, the decent degradation of the organic molecules was found. This difficulty could be overcome by applying a higher intensity light. Hence, the photocatalytic degradation efficiency could be enhanced with hiking the intensity of incident light [31]. Therefore, accelerated photocatalytic degradation could be found with a higher intensity of sunlight.

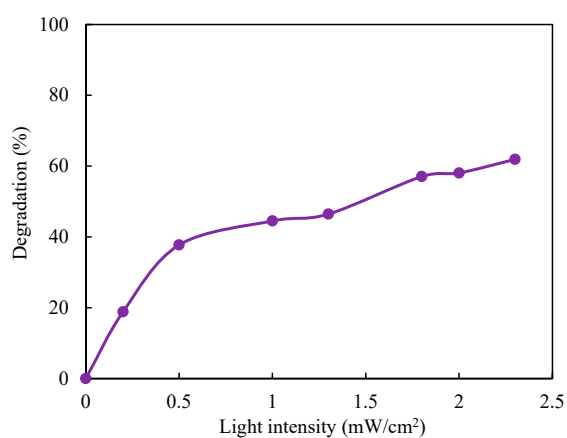


**Figure 6.** Influence of light intensity on the photocatalytic picloram degradation in existence of  $\text{TiO}_2$  under sunlight. Picloram: 20 ppm;  $\text{TiO}_2$ : 300 mg; irradiation time: 10 min; pH: 4 and temperature:  $30^\circ\text{C}$ .

### 3.5. Influence of Temperature

The photocatalytic picloram degradation could be influenced by the temperature and the influence was investigated by changing the temperature from 10 to 60 °C. The reaction solution was irradiated for 10 min under sunlight to find the influence of the reaction temperature, since the picloram was not completely degraded within 10 min. Figure 7 shows the results. The degradation efficiency of picloram tended to raise slowly as the reaction temperature hiked, and the similar phenomena are recorded in other researches [32]. This result confirmed the higher degradation efficiency of picloram at a higher temperature. However, the high-energy cost may be required to raise the temperature during the practical application. Hence, the reaction temperature was fixed to 30 °C to minimize the extra treatment cost.

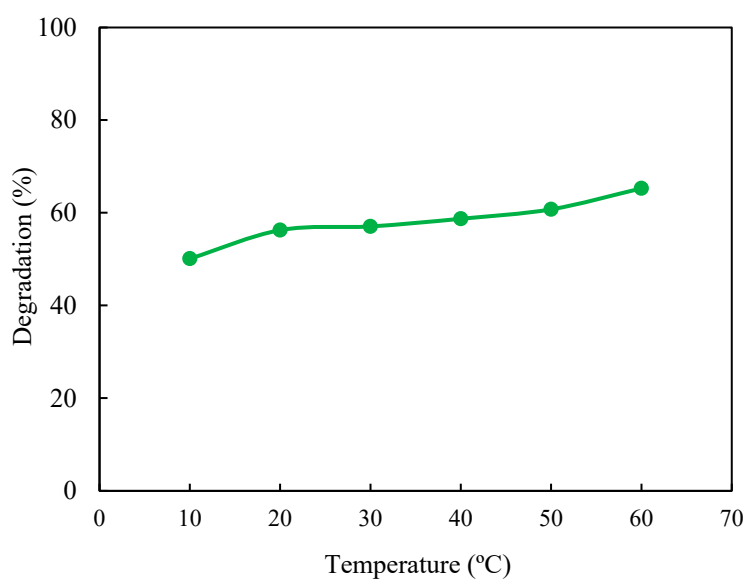


**Figure 7.** Influence of temperature on the photocatalytic picloram degradation in existence of TiO<sub>2</sub> under sunlight. Picloram: 20 ppm; TiO<sub>2</sub>: 300 mg; irradiation time: 10 min; pH: 4 and intensity of light: 1.8 mW/cm<sup>2</sup>.

### 3.6. Influence of Irradiation Time

The influence of the irradiation time of sunlight on the photocatalytic degradation of picloram was investigated, keeping other parameters constant. The results are shown in Figure 8a. The photocatalytic degradation efficiency of the picloram was sharply raised with rising irradiation time in the presence TiO<sub>2</sub>. However, no significant degradation was recorded without TiO<sub>2</sub>. The degradation rate was elevated to 100% with 300 mg of TiO<sub>2</sub> within 30 min at 30 °C. In addition, these results explained the molecular structure of the picloram was totally broken after 30 min of light irradiation. The interaction of picloram molecule with TiO<sub>2</sub> surface can be increased owing to the increased irradiation time. Therefore, the photocatalytic degradation efficiency of picloram was increased [33].

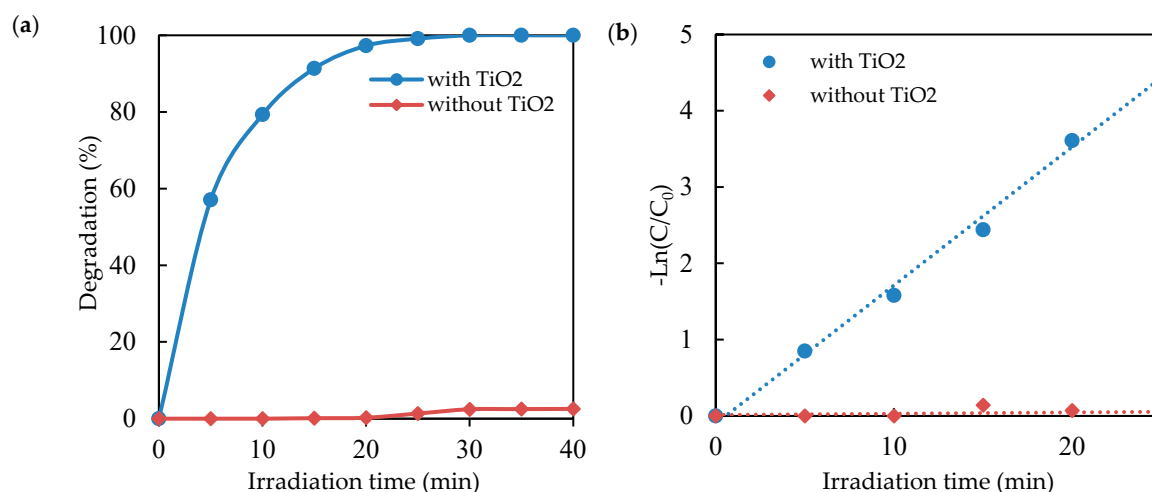


**Figure 8.** (a) Influence of irradiation time on the photocatalytic picloram degradation in existence of  $\text{TiO}_2$  under sunlight; (b) Plot of  $-\ln(C/C_0)$  vs. irradiation time. Picloram: 20 ppm;  $\text{TiO}_2$ : 300 mg; pH: 4; intensity of light:  $1.8 \text{ mW/cm}^2$  and temperature:  $30 \text{ }^\circ\text{C}$ .

### 3.7. Kinetics

The Langmuir-Hinshelwood (L-H) model was implemented to study the kinetics of photocatalytic degradation of picloram [34]. The photocatalytic degradation of picloram with  $\text{TiO}_2$  is aligned to the Langmuir-Hinshelwood (L-H) theory and is shown in Equation (2):

$$r = -\frac{dC}{dt} = \frac{kKC}{1 + KC} \quad (2)$$

where  $r$  ( $\text{mg/L min}$ ) is the degradation rate of the picloram,  $K$  ( $\text{L/g}$ ) is the adsorption co-efficient,  $k$  ( $\text{min}^{-1}$ ) is the rate constant, and  $C$  ( $\text{mg/L}$ ) is the substrate concentration.

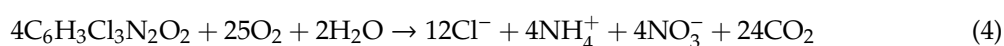
Equation (3) can be written by simplifying Equation (2) for a very small initial concentration ( $C_0$ ) of substrate, and shows a linear expression of  $\ln(C/C_0)$  versus irradiation time  $t$ ; here,  $k_{app}$  is the first-order reaction rate constant.

$$-\ln\left(\frac{C}{C_0}\right) = kKt = k_{app}t \quad (3)$$

Thus, to ensure the hypothesis,  $-\ln(C/C_0)$  was plotted against the irradiation time ( $t$ ) for the photocatalytic degradation and photolysis (without  $\text{TiO}_2$ ) of the picloram. The photocatalytic picloram degradation kinetics concluded the pseudo-first-order kinetics owing to obtaining the strong linear relations, shown in Figure 8b. The pseudo-first-order rate constants for photocatalytic degradation of picloram was  $17.6 \times 10^{-2} \text{ min}^{-1}$  with 4 min of reaction half-life. The kinetic results proved the photocatalytic picloram degradation with  $\text{TiO}_2$  was very effective since it was proceeded by the photolytic degradation of the picloram.

### 3.8. Mineralization

Picloram was fully decomposed in the presence of  $\text{TiO}_2$  after 30 min solar of irradiation, as shown in Figure 9. Several intermediates of picloram could be detected during the degradation process. These obtained intermediates may be toxic. Therefore, the mineralization of the picloram has been investigated. Probably, chloride, ammonium and nitrate ions and  $\text{CO}_2$  could be found as the final products of picloram. Here, a contemplate equation is presented for the total mineralization reaction of the picloram aqueous solution with nanosized  $\text{TiO}_2$ .





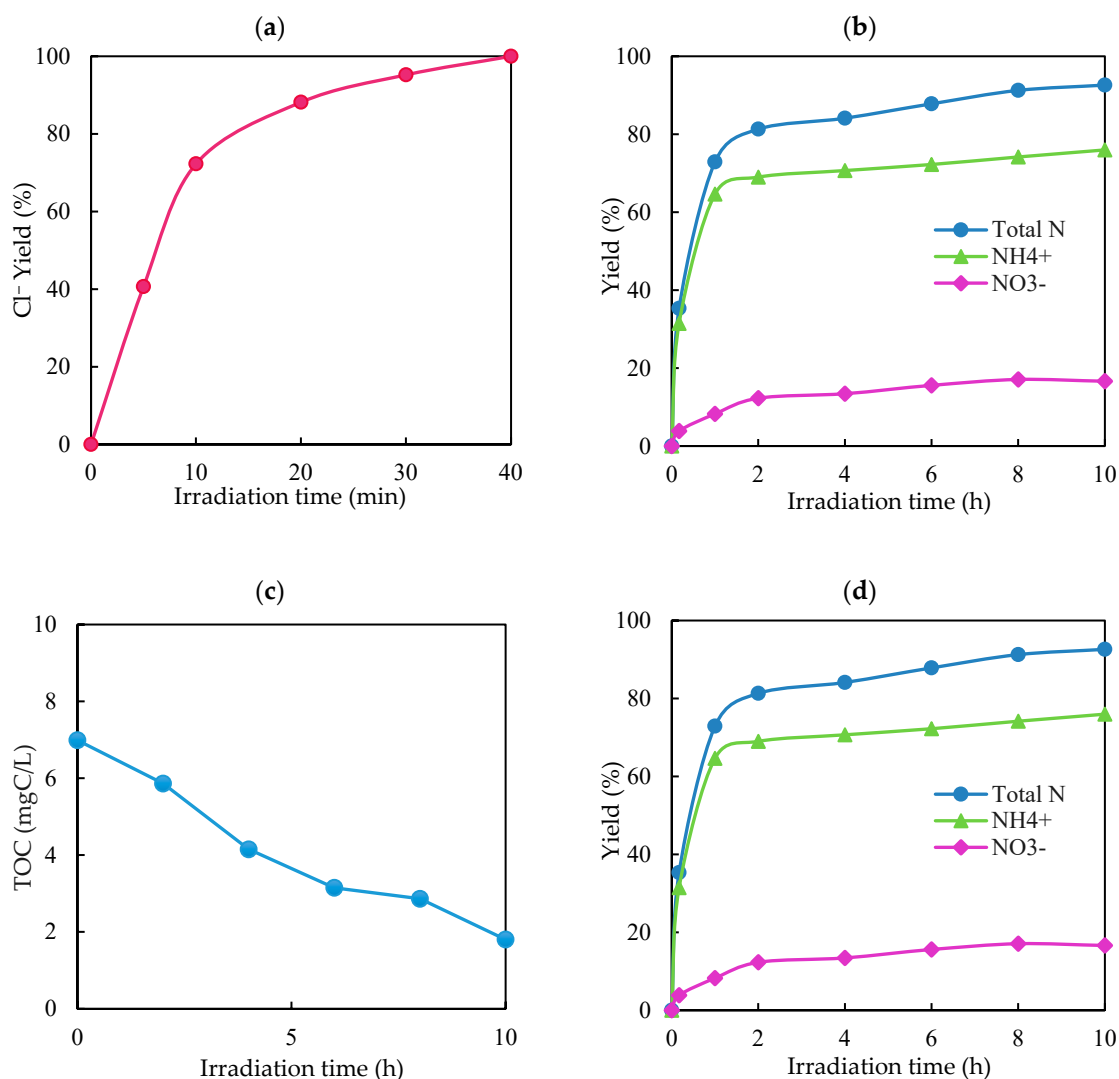


**Figure 9.** Mineralization of picloram solution in existence of TiO<sub>2</sub> under sunlight. (a) formation of Cl<sup>-</sup> ion; (b) formation of NH<sub>4</sub><sup>+</sup> ions and NO<sub>3</sub><sup>-</sup> ions; (c) removal of total organic carbon (TOC), and (d) formation of HCOOH. Picloram: 20 ppm; TiO<sub>2</sub>: 300 mg; pH: 4; intensity of light: 1.8 mW/cm<sup>2</sup> and temperature: 30 °C.

The amounts of chloride, ammonium and nitrate ions during photocatalytic picloram degradation were measured by an ion chromatography. Carbon mineralization, associated with the generation of CO<sub>2</sub>, was scrutinized by measuring the total organic carbon (TOC).

Initially, the chloride ion evolution was estimated in the existence of TiO<sub>2</sub> nanoparticles. The produced chloride ion yield was increased with the irradiation time, as seen in Figure 9a. The chloride ion yield was 95% after 30 min of irradiation. The chlorine atom in picloram was completely mineralized within 40 min of irradiation.

The theoretical total amount of ammonium and nitrate ions was 0.166 mmol/L, when 50 mL of 20 ppm picloram aqueous solution was completely mineralized. Figure 9b explained that the yields of ammonium ion and nitrate ions raised with the irradiation time, and the yield was 92% after 10 h of solar irradiation. The production amount of ammonium ion decreased sharply from around 1 h of light irradiation. Figure shows it that the yield of ammonium ions started to decrease, when the yield of nitrogen atom was approximately 50%. Picloram contains two nitrogen atoms, one in pyridine ring (-N-) and another as an amino group (-NH<sub>2</sub>). The initial linear increase occurred due to the

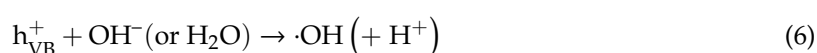
elimination of amino group from the picloram molecule and later N atom in pyridine ring can be mineralized. The same results have already been shown in the photocatalytic decomposition of nitrogen containing organic compounds. Then, the decrease in total organic carbon (TOC) during photocatalytic degradation of picloram was examined (Figure 9c). The TOC of the picloram solution decreased by 74% after 10 h, which demonstrated that CO<sub>2</sub> was generated from the dissolved carbon during the photocatalytic picloram degradation in the presence of TiO<sub>2</sub>. However, the remaining TOC could decrease during further light irradiation.

The picloram degradation largely depends on the elimination of the substituent on the pyridine ring. Generally, picloram contains carboxylic (-COOH), chloride (-Cl) and amino groups (-NH<sub>2</sub>). Therefore, the formation of formic acid was expected because of the elimination of the carboxylic group during the photocatalytic picloram degradation. The formation was confirmed by the high performance liquid chromatography. Figure 9d shows the produced amount of formic acid was increased initially, and later decreased with the irradiation time. The progress of oxidative degradation of the picloram into various compounds by photocatalysis can continue with formic acid formation.

### 3.9. Identification of Photoproducts and Photocatalytic Degradation Mechanism

The intermediate products, which were produced during the photocatalytic degradation of the picloram aqueous solution with TiO<sub>2</sub>, were identified by GC/MS analysis after 10 min and 30 min of solar irradiation. The picloram was confirmed by the obtained peak with the retention time of 17.0 min compared with the mass spectrum of the NIST library (Figure S1). However, it was not possible to confirm a substance as a degradation intermediate of picloram from the chromatograms after 10 min and 30 min of sunlight irradiation. Therefore, the degradation mechanism was explained by theoretical calculation since it was not possible to identify the decomposition intermediate by GC-MS.

The point charge and the frontier electron density helped to understand the degradation mechanism of the picloram. The MOPAC simulation value was shown in Table 2. Accordingly, the frontier electrons were more relatively distributed on the carbon atoms of the pyridine ring rather than the substituents. Therefore, the atoms of the 6-membered pyridine ring were easily attacked by hydroxyl radical causing substitution reactions. Especially, Cl atom-containing carbons, C(3) and C(5) are considered to be particularly susceptible to attack by hydroxyl radical. Again, N and O atoms have a particularly high negative point charge. As mentioned earlier, the TiO<sub>2</sub> surface is positively charged on the acidic condition and negatively charged on the basic condition. Therefore, the surface of TiO<sub>2</sub> was positively charged since the pH of the picloram solution was four. It was assumed that the picloram was adsorbed on TiO<sub>2</sub> at the sites of amino and carboxyl groups. Based on the present study and other literature reports, the plausible mechanism for photocatalytic picloram degradation with TiO<sub>2</sub> nanoparticles under sunlight would be exhibited in Scheme 1. Conventionally, most of the organic pollutants were degraded under sunlight in the presence of favorable metal oxide-based semiconductor photocatalysts. The suitable bandgap of TiO<sub>2</sub> nanoparticles (E<sub>g</sub> ≈ 3.2 eV) prefers the absorption of the photons with energy, which are greater than the bandgap energy. Similarly, TiO<sub>2</sub> can be agitated to form electrons-holes in the valence band (VB) under light irradiation. The excited electrons are migrated toward the conduction band (CB), while holes are remained in valence band under sunlight [35] (Equation (5)). The valence band holes, h<sub>VB</sub><sup>+</sup> could attack the oxidizing species like H<sub>2</sub>O and OH<sup>-</sup> to generate hydroxyl radical (•OH) (Equation (6)), and alternatively, the conduction band electrons can be trapped by the reducing species (namely O<sub>2</sub> and H<sub>2</sub>O<sub>2</sub>) obtained from the reaction solution to produce superoxide radicals (•O<sub>2</sub><sup>-</sup>) or hydroperoxyl radicals (•OOH) on the surface of TiO<sub>2</sub> [36,37] (Equations (7)–(10)). These generated radicals can decompose picloram into chloride, ammonium and nitrate ions and CO<sub>2</sub> in aqueous solution (Equation (11)).



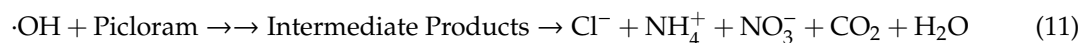
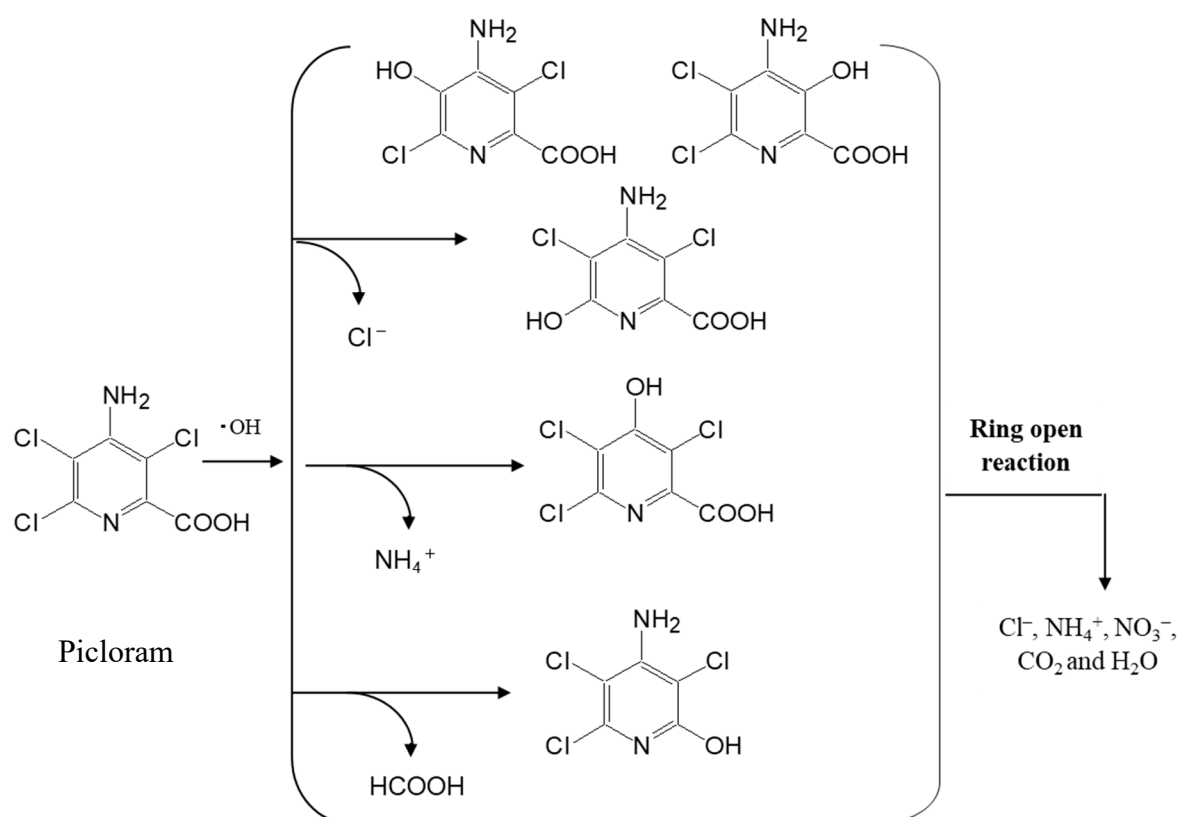


**Table 2.** Calculation of the frontier electron density (FED) and point charge (PC) of the picloram.

Atom	Frontier Electron Density (FED)	Point Charge (PC)	Atom	Frontier Electron Density (FED)	Point Charge (PC)
N(1)	0.149	-0.128	Cl(9)	0.032	0.049
C(2)	0.261	0.023	Cl(10)	0.077	0.024
C(3)	0.351	-0.126	C(11)	0.044	0.357
C(4)	0.117	0.155	O(12)	0.047	-0.338
C(5)	0.349	-0.153	O(13)	0.010	-0.259
C(6)	0.169	0.047	H(14)	0	0.258
N(7)	0.335	-0.418	H(15)	0	0.259
Cl(8)	0.059	0.005	H(16)	0	0.245



**Scheme 1.** The plausible mechanism of the photocatalytic picloram degradation in the existence of  $TiO_2$  under sunlight.

#### 4. Conclusions

The present study confirmed the photocatalytic picloram degradation in the presence of  $TiO_2$  under sunlight. The  $TiO_2$  nanoparticles is considered to be an effective photocatalyst and simply

applied to detoxify the picloram-contaminated water. The optimum conditions for instance, TiO<sub>2</sub> dosage, initial solution pH, intensity of light, reaction temperature and irradiation time of sunlight was determined from the solar photocatalytic picloram degradation. The TiO<sub>2</sub> amount: 300 mg; temperature: 30 °C; pH: 4; light intensity: 1.8 mW/cm<sup>2</sup> and irradiation time: 10 min are the optimum conditions. The pseudo-first-order reaction kinetics was confirmed following the Langmuir-Hinshelwood model, with a reaction rate constant of  $17.6 \times 10^{-2} \text{ min}^{-1}$ . The degradation of picloram using TiO<sub>2</sub> is maintained an oxidative reaction by radical species including hydroxyl radicals (•OH). Picloram is photo-degradable under sunlight, and the introduction of TiO<sub>2</sub> could immensely enhance the photocatalytic degradation of the picloram. Finally, picloram is perfectly mineralized into inorganic ions such as chloride, ammonium, nitrate ions, and CO<sub>2</sub> as the end products. Therefore, the study could be considered to be a practical application for the remediation of the picloram in the future.

**Supplementary Materials:** The following are available online at <http://www.mdpi.com/2305-7084/4/4/58/s1>, Figure S1a: GC-MS-EI total ion chromatogram obtained for a SPE extraction of picloram solution, Figure S1b: GC-MS-EI total ion chromatogram obtained for a SPE extraction of picloram solution after 10 min irradiation, Figure S1c: GC-MS-EI total ion chromatogram obtained for a SPE extraction of picloram solution after 30 min of irradiation, Table S1: Analytical conditions for ion chromatography to determine NH<sub>4</sub><sup>+</sup> ion, Table S2: Analytical conditions for ion chromatography to determine Cl<sup>-</sup> and NO<sub>3</sub><sup>3-</sup> ion, Table S3: Analytical conditions to determine the formation of formic acid.

**Author Contributions:** M.R.I. wrote the manuscript, J.B.I. and S.K. conceived, designed and wrote the experiments. J.B.I. performed the experiments and wrote the manuscript. I.T., M.F. and H.K. analyzed the results and advised the project. All authors have read and agreed to the published version of the manuscript.

**Funding:** The current work was partly funded by the Ministry of Education, Culture, Sports, Science, and Technology, Japan under the Grant-in-Aid for Scientific Research (C) 18K11709.

**Acknowledgments:** All the experiments were performed at Mie University. Any opinions, findings, conclusions or recommendations shared in this article are those of the authors and do not undoubtedly contemplate the view of the supporting organizations.

**Conflicts of Interest:** The authors declare no conflict of interest.

## References

1. Ghauch, A. Degradation of Benomyl, Picloram, and Dicamba in a Conical Apparatus by Zero-Valent Iron Powder. *Chemosphere* **2001**, *43*, 1109–1117. [[CrossRef](#)]
2. Rahman, M.A.; Muneer, M. Heterogeneous Photocatalytic Degradation of Picloram, Dicamba, and Floumeturon in Aqueous Suspensions of Titanium Dioxide. *J. Environ. Sci. Health* **2005**, *40*, 247–267. [[CrossRef](#)] [[PubMed](#)]
3. Ozcan, A.; Sahin, Y.; Koparal, A.S.; Oturan, M.A. Degradation of Picloram by the Electro-Fenton Process. *J. Hazard. Mater.* **2008**, *153*, 718–727. [[CrossRef](#)] [[PubMed](#)]
4. Sadowsky, M.J.; Koskinen, W.C.; Bischoff, M.; Barber, B.L.; Becker, J.M.; Turco, R.F. Rapid and Complete Degradation of the Herbicide Picloram by *Lipomyces Kononenkoae*. *Agric. Food Chem.* **2009**, *57*, 11. [[CrossRef](#)] [[PubMed](#)]
5. Wells, M.J.M.; Yu, L.Z. Solid-Phase Extraction of Acidic Herbicides. *J. Chromatogr. A* **2000**, *885*, 237–250. [[CrossRef](#)]
6. Pereira, G.F.; Rocha-Filho, R.C.; Bocchi, N.; Biaggio, S.R. Electrochemical Degradation of the Herbicide Picloram Using a Filter-Press Flow Reactor with a Boron-doped Diamond or  $\beta$ -PbO<sub>2</sub> Anode. *Electrochimica Acta* **2015**, *179*, 588–598. [[CrossRef](#)]
7. Burns, C.J.; Swaen, G.M.H. Review of 2,4-dichlorophenoxyacetic acid (2,4-D) biomonitoring and epidemiology. *Crit. Rev. Toxicol.* **2012**, *42*, 768–786. [[CrossRef](#)]
8. Tu, M.; Hurd, C.; Randall, J.M. *Weed Control Methods Handbook: Tools & Techniques for Use in Natural Areas*; The Nature Conservancy: Arlington, VA, USA, 2001; Chapter 7.
9. Passos, A.B.R.J.; Souza, M.F.; Silva, D.V.; Saraiva, D.T.; Silva, A.A.; Zanuncio, J.C.; Gonçalves, B.F.S. Persistence of Picloram in Soil with Different Vegetation Managements. *Environ. Sci. Pollut. Res.* **2018**, *25*, 23986–23991. [[CrossRef](#)]

10. Teixeira, S.C.G.; Canela, M.C. Degradation of Padron<sup>®</sup> by Photochemical Processes Using Artificial and Sunlight Radiation. *Quim. Nova.* **2007**, *30*, 1830–1834. [[CrossRef](#)]
11. Pratap, K.; Lemley, A.T. Electrochemical Peroxide Treatment of Aqueous Herbicide Solutions. *J. Agric. Food Chem.* **1994**, *42*, 209–215. [[CrossRef](#)]
12. Chamberlain, E.; Shi, H.; Wang, T.; Ma, Y.; Fulmer, A.; Adams, C. Comprehensive Screening Study of Pesticide Degradation via Oxidation and Hydrolysis. *J. Agric. Food Chem.* **2012**, *60*, 354–363. [[CrossRef](#)]
13. Vranjes, M.; Saponjic, Z.V.; Zivkovic, L.S.; Despotovic, V.N.; Sojic, D.V.; Abramovic, B.F.; Comor, M.I. Elongated Titania Nanostructures as Efficient Photocatalysts for Degradation of Selected Herbicides. *Appl. Catal. B* **2014**, *589*, 160–161. [[CrossRef](#)]
14. Reinhold, D.; Vishwanathan, S.; Park, J.J.; Oh, D.; Saunders, F.M. Assessment of Plant-Driven Removal of Emerging Organic Pollutants by Duckweed. *Chemosphere* **2010**, *80*, 687–692. [[CrossRef](#)] [[PubMed](#)]
15. Ordaz-Guillén, Y.; Galíndez-Mayer, C.J.; Ruiz-Ordaz, N.; Juárez-Rameirez, C.; Santoyo-Tepole, F.; Ramos-Monroy, O. Evaluating the Degradation of the Herbicides Picloram and 2,4-D in a Compartmentalized Reactive Biobarrier with Internal Liquid Recirculation. *Environ. Sci. Pollut. Res.* **2014**, *21*, 8765–8773. [[CrossRef](#)]
16. Yang, J.K.; Lee, S.M. Removal of Cr(VI) and Humic Acid by Using TiO<sub>2</sub> Photocatalysis. *Chemosphere* **2006**, *63*, 1677–1684. [[CrossRef](#)]
17. Islam, J.B.; Furukawa, M.; Tateishi, I.; Katsumata, H.; Kaneco, S. Photocatalytic Reduction of Hexavalent Chromium with Nanosized TiO<sub>2</sub> in Presence of Formic Acid. *ChemEngineering* **2019**, *3*, 33. [[CrossRef](#)]
18. Qi, H.; Wang, S.; Liu, H.; Gao, Y.; Wang, T.; Huang, Y. Synthesis of an Organic–Inorganic Polypyrrole/Titanium(IV) Biphosphate Hybrid for Cr(VI) Removal. *J. Mol. Liq.* **2016**, *215*, 402–409. [[CrossRef](#)]
19. Joubani, M.N.; Siboni, M.S.; Yang, J.K.; Gholami, M.; Farzadkia, M. Photocatalytic Reduction of Hexavalent Chromium with Illuminated ZnO/TiO<sub>2</sub> Composite. *J. Ind. Eng. Chem.* **2015**, *22*, 317–323. [[CrossRef](#)]
20. Islam, J.B.; Furukawa, M.; Tateishi, I.; Katsumata, H.; Kaneco, S. Formic Acid Motivated Photocatalytic Reduction of Cr(VI) to Cr(III) with ZnFe<sub>2</sub>O<sub>4</sub> Nanoparticles Under UV Irradiation. *Environ. Technol.* **2020**. [[CrossRef](#)]
21. Chu, D.W.; Masuda, Y.; Ohji, T.; Kato, K. Formation and Photocatalytic Application of ZnO Nanotubes Using Aqueous Solution. *Langmuir* **2010**, *26*, 2811–2815. [[CrossRef](#)]
22. Samad, A.; Ahsan, S.; Tateshi, I.; Furukawa, M.; Katsumata, H.; Suzuki, T.; Kaneco, S. Indirect Photocatalytic Reduction of Arsenate to Arsenite in Aqueous Solution with TiO<sub>2</sub> in the Presence of Hole Scavengers. *Chin. J. Chem. Eng.* **2018**, *26*, 529–533. [[CrossRef](#)]
23. Islam, J.B.; Furukawa, M.; Tateishi, I.; Kawakami, S.; Katsumata, H.; Kaneco, S. Enhanced Photocatalytic Reduction of Toxic Cr(VI) with Cu Modified ZnO Nanoparticles in Presence of EDTA Under UV Illumination. *SN Appl. Sci.* **2019**, *1*, 1240–1250. [[CrossRef](#)]
24. Lee, D.J.; Senseman, S.A.; Sciumbato, A.S.; Jung, S.C.; Krutz, L.J. The effect of Titanium Dioxide alumina Beads on the Photocatalytic Degradation of Picloram in Water. *J. Agric. Food Chem.* **2003**, *51*, 2659–2664. [[CrossRef](#)] [[PubMed](#)]
25. Abramovic, B.; Sojic, D.; Despotovic, V.; Vione, D.; Pazzi, M.; Csanadi, J. A Comparative Study of the Activity of TiO<sub>2</sub> Wackherr and Degussa P25 in the Photocatalytic Degradation of Picloram. *Appl. Catal. B* **2011**, *105*, 191–198. [[CrossRef](#)]
26. Aramendía, M.A.; Colmenares, J.C.; López-Fernández, S.; Marinas, A.; Marinas, J.M.; Moreno, J.M.; Urbano, F.J. Photocatalytic Degradation of Chlorinated Pyridines in Titania Aqueous Suspensions. *Catal. Today* **2008**, *138*, 110–116. [[CrossRef](#)]
27. Islam, J.B.; Furukawa, M.; Tateishi, I.; Katsumata, H.; Kaneco, S. Photocatalytic Degradation of a Typical Neonicotinoid Insecticide: Nitenpyrum by ZnO Nanoparticles under Solar Irradiation. *Environ. Sci. Pollut. Res.* **2020**, *27*, 20446–20456. [[CrossRef](#)]
28. Coleman, H.M.; Vimonses, V.; Leslie, G.; Amal, R. Degradation of 1, 4-Dioxane in Water Using TiO<sub>2</sub> Based Photocatalytic and H<sub>2</sub>O<sub>2</sub>/UV Processes. *J. Hazard. Mater.* **2007**, *146*, 496–501. [[CrossRef](#)] [[PubMed](#)]
29. Molla, M.A.I.; Furukawa, M.; Tateishi, I.; Katsumata, H.; Kaneco, S. Mineralization of Diazinon with Nanosized-Photocatalyst TiO<sub>2</sub> in Water under Sunlight Irradiation: Optimization of Degradation Conditions and Reaction Pathway. *Environ. Technol.* **2019**. [[CrossRef](#)]

30. Molla, M.A.I.; Furukawa, M.; Tateishi, I.; Katsumata, H.; Kaneco, S. Solar Photocatalytic Decomposition of Probenazole in Water with TiO<sub>2</sub> in the Presence of H<sub>2</sub>O<sub>2</sub>. *Energy Source Part. A* **2018**, *40*, 2432–2441. [[CrossRef](#)]
31. Gnanaprakasam, A.; Sivakumar, V.M.; Thirumarimurugan, M. Influencing Parameters in the Photocatalytic Degradation of Organic Effluent via Nanometal Oxide Catalyst: A Review. *Indian J. Eng. Mater. Sci.* **2015**, 601827. [[CrossRef](#)]
32. Islam, J.B.; Furukawa, M.; Tateishi, I.; Katsumata, H.; Kaneco, S. Photocatalytic Degradation of a Typical Agricultural Chemical: Metalaxyl in Water using TiO<sub>2</sub> under Solar Irradiation. *SN Appl. Sci.* **2020**, *2*, 925. [[CrossRef](#)]
33. Kumar, A.; Pandey, G. The photocatalytic Degradation of Methyl Green in Presence of Visible Light with Photoactive Ni 0.10: La 0.05: TiO<sub>2</sub> Nanocomposites. *IOSR-JAC* **2017**, *10*, 31–44. [[CrossRef](#)]
34. Turchi, C.S.; Ollis, D.E. Photocatalytic Degradation of Organic Water Contaminants: Mechanisms Involving Hydroxyl Radical Attack. *J. Catal.* **1990**, *122*, 178–192. [[CrossRef](#)]
35. Fotiou, T.; Triantis, T.; Kaloudis, T.; Hiskia, A. Photocatalytic Degradation of Cyindrospermopsin under UV-A, Solar and Visible Light using TiO<sub>2</sub>. Mineralization and Intermediate Products. *Chemosphere* **2015**, *119*, 89–94. [[CrossRef](#)] [[PubMed](#)]
36. Zhao, C.; Pelaez, M.; Dionysiou, D.D.; Pillai, S.C.; Byrne, J.A.; O’Shea, K.E. UV and Visible Light Activated TiO<sub>2</sub> Photocatalysis of 6-Hydroxymethyl Uracil, A Model Compound for the Potent Cyanotoxin Cyindrospermopsin. *Catal. Today* **2014**, *224*, 70–76. [[CrossRef](#)]
37. Antoniou, M.G.; Zhao, C.; O’Shea, K.E.; Zhang, G.; Dionysiou, D.D.; Zhao, C.; Han, C.; Nadagouda, M.N.; Choi, H.; Fotiou, T.; et al. Chapter 1: Photocatalytic Degradation of Organic Contaminants in Water: Process Optimization and Degradation Pathways. In *Photocatalysis: Applications*; RSC Energy and Environment Series No. 15; Royal Society of Chemistry Publishing: Cambridge, UK, 2016; pp. 1–34. [[CrossRef](#)]

**Publisher’s Note:** MDPI stays neutral with regard to jurisdictional claims in published maps and institutional affiliations.



© 2020 by the authors. Licensee MDPI, Basel, Switzerland. This article is an open access article distributed under the terms and conditions of the Creative Commons Attribution (CC BY) license (<http://creativecommons.org/licenses/by/4.0/>).